

The Issue of Strouhal Number Definition in Cavitating Flow

Matevž Dular^{1,*} - Rudolf Bachert²

¹University of Ljubljana, Faculty of Mechanical Engineering, Slovenia

²AUMA Reister GmbH & Co. KG, Germany

In the past years the Strouhal number has been used to define the nature of cavitation cloud shedding in many studies. In particular, it was adopted as an indicator of a simulation agreement to the experiment. The problem is that there are many interpretations of the parameters that are included in its definition, which leads to a confusion and, as this study shows, to its uselessness. Literature was surveyed and Strouhal numbers with different definitions for several well-defined experiments were calculated. The span of the results exceeded one order of magnitude. The results are discussed and finally, a proposal for a unification of the definition of the Strouhal number is given.

© 2009 Journal of Mechanical Engineering. All rights reserved.

Keywords: cavitation, Strouhal number, PIV, high-speed visualization

0 INTRODUCTION

The Strouhal number is used by an analysis of unsteady, oscillating flow problems. It represents a measure of the ratio of inertial forces due to the unsteadiness of the flow or local acceleration to the inertial forces due to changes in velocity from one point to another in the flow field. It is defined as:

$$Str = \frac{f \cdot l}{v}, \quad (1)$$

where f is the characteristic oscillation frequency, l is the characteristic length and v is the characteristic flow velocity.

In developed cavitating flow cavitation clouds separate from the attached part of the cavity and travel downstream until the point of their collapse (Fig. 1).

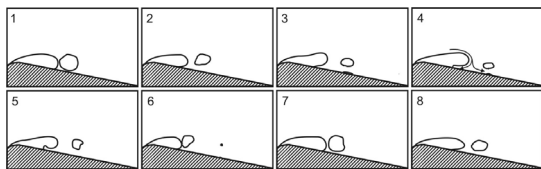


Fig. 1. *The schematic sequence showing cavitation cloud shedding*

One period of cloud shedding begins with slow growth of the attached part of the cavity. At its closure, reentrant jet forms that flows upstream and consequently causes the cavitation cloud to separate (at this point the maximum size of the attached part of the cavity is reached). While the separated cloud flows downstream and collapses

in the higher pressure region the attached cavity begins to grow again and the process is repeated.

The cavitation cloud shedding frequency can be relatively simply and accurately measured and is therefore, a well-defined parameter of cavitation behavior. Since the frequency by itself cannot be compared between the experiments, many authors adopted the nondimensional Strouhal number for the evaluation of the dynamic behavior of the developed cavitation. It is generally acknowledged that the value of the Strouhal number for a developed cavitating flow lies in the range between 0.2 and 0.5.

However, together with the apparently straightforward definition problems arose. Different authors chose different definitions for the characteristic quantities, so a relatively vast span of Strouhal numbers can be calculated for each experiment. It also occurs that authors do not share the definitions of the variables at all (Kunz et al. [1], Kawamura and Sakoda [2], Hosangadi and Ahuja [3]). This inconsistency devaluates the meaning of the Strouhal number and calls for the unification of the definitions of the variables of frequency, length and velocity that define it.

The paper first discusses each of the variables in the definition of the Strouhal number for cavitating flow and gives references to different interpretations. The second part gives a description of a set of experiments where high speed visualization and PIV (Particle Image Velocimetry) were used to determine the Strouhal number according to all known interpretations of frequency, length and velocity. In the discussion an overview of all the possibilities of calculating

the Strouhal number and comments on the vast span of obtained values are presented. Finally, a suggestion for the unification of the definitions of variables, which gives the most accurate value of Strouhal number, is proposed.

1 INTERPRETATIONS

In this section definitions of characteristic frequency, length and velocity are discussed.

1.1 The Characteristic Frequency

Among the three variables that define the Strouhal number the characteristic frequency is the least problematic to define. Naturally, all authors define it as the cavitation cloud separation frequency that can easily be determined with high speed visualization, dynamic pressure measurements, lift measurements, LDA (Laser Doppler Velocimetry), time resolved PIV or some other method. Usually these methods all produce comparable results although Saito et al. [4] reported big discrepancies in frequencies in a specific range of cavitation numbers when defined by dynamic pressure measurements or by lift coefficient measurements.

1.2 The Characteristic Length

Characteristic length is the most problematic quantity in the Strouhal number. Not only are there numerous definitions for it, but it is in some cases also very hard to measure it precisely. When it is related to the cavitation structure and not to some other constant geometrical dimension, the only way to determine it experimentally is by visual observation.

If we concentrate only on the developed cavitation on a single hydrofoil we can find the following definitions for the characteristic length (Fig. 2).

1.2.1 The Correct Value l_{cc}

The most appropriate length scale is the mean length of the separated cloud just after the separation l_{cc} . This reference length is usually, but not necessarily, almost the same as the length to which the attached cavity grows before the cavitation cloud separates, Franc [5]. The problem of using the length of the almost

separated cavitation cloud l_{cc} as the characteristic length is its very hard and expensive measurement. For an accurate evaluation of its magnitude, a visual access and a high speed camera are needed, making the l_{cc} a very unfavorable parameter.

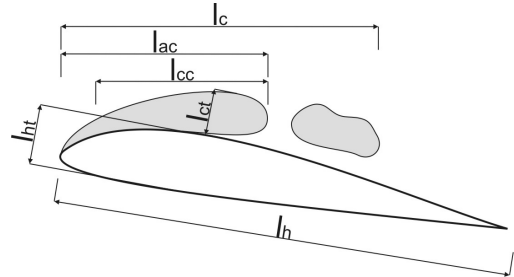


Fig. 2. Interpretations for the characteristic length

1.2.2 The Length of the Hydrofoil l_h

This dimension is very easy to measure and, therefore, practical to use. The problem is that it is only indirectly related to the length scale at which cavitation cloud shedding takes place – one can claim that the scale will increase proportionally with the size of the geometry in question. It was adopted by the following authors Saito et al. [4], Duttweiler and Brennen [6], Schnerr and Sauer [7], Iga et al. [8], Sato et al. [9] and Song and Qin [10].

1.2.3 The Maximum Thickness of the Hydrofoil l_{ht}

Apart from the fact that it is easy to determine, the thickness of the hydrofoil has little perspective in definition of the Strouhal number. It is even hard to claim that the length scales of cavitation cloud shedding and foil thickness are proportional. This dimension was used by Berntsen et al. [11].

1.2.4 The Mean Cavity Thickness l_{ct}

Ceccio & Brennen [12] proposed the use of the mean thickness of the cavity as the characteristic length. It is only possible to measure it when visual observation of cavitation is enabled. This dimension is related to the length scale of cavitation cloud shedding (apart from averaging) and, therefore, appropriate to use. A problem is that after averaging the attached cavity and the separated cavitation the cloud cannot be

distinguished any more and the proportionality of the length scales of the thickness and the cloud shedding can again become questionable.

Further issues of this method are also the uncertainty of measurement due to small size and determining the boundary between the cavitation structure and the pure liquid flow (even more so if we are observing a time averaged cavitation structure).

1.2.5 The Mean Cavity Length l_c

The problem of uncertainty of the measurement of cavity means that thickness can be somewhat reduced when the mean cavity length is observed (as it is larger in size). On the other hand, this method is even more bound to the fact that the attached cavity and the separated clouds cannot be distinguished, which can lead to unproportional length scales. Despite this, this approach is commonly used - among others by Bachert et al. [13], Frobenius et al. [14], Stutz and Reboud [15] and Maître and Pellone [16].

1.2.6 The Mean Length of the Attached Part of the Cavity l_{ac}

This approach requires the use of phase averaging. When only situations just before the cavitation cloud separations are observed, the attached and the separated vapor structure can easily be distinguished and the appropriate length scale can be determined. This, the most accurate, approach (apart from measuring the mean length of the separated cloud) has been used by many authors: Saito et al. [4], Franc [5], Iga et al. [8], Caron et al. [17], Coutier-Delgosha et al. [18], de Lange et al. [19], Leroux et al. [20], Callenaere et al. [21], Laberteaux and Ceccio [22], Reboud et al. [23], Hofmann et al. [24] and de Lange and de Bruin [25].

1.3 The Characteristic Velocity

Similarly to the question of the appropriate length scale, the issue of characteristic velocity is difficult to address.

1.3.1 The Correct Value v_{rj}

The most accurate measure would be to use the reentrant jet velocity at the closure of the attached cavity just before the cavitation cloud

separates v_{rj} – a fair approximation (according to the potential flow theory) would be the velocity near the attached cavity closure point at the interface between the vapor structure and the pure liquid flow. It is meaningless to describe the complexity of the measurements required to determine these velocities, but some authors did just that, while others used simpler approaches. Fig. 3 shows several definitions of characteristic velocity that are discussed in the following text.

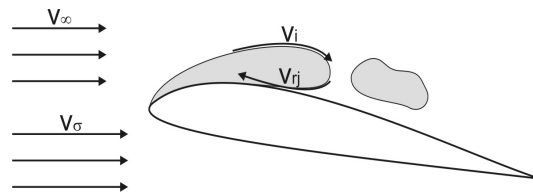


Fig. 3. Interpretations of the characteristic velocity

1.3.2 Free Stream Velocity v_∞

The simplest to determine and most accurate to measure is the velocity upstream of the hydrofoil. Its use is just since it is quite possibly closely related to the velocity that causes cavitation cloud separation. It is also the most common (almost the only) characteristic velocity that is found in literature (Saito et al. [4], Franc [5], Duttweiler and Brennen [6], Schnier & Sauer [7], Iga et al. [8], Sato et al. [9], Song and Qin [10], Berntsen et al. [11], Ceccio and Brennen [12], Stutz and Reboud [15], Maître and Pellone [16], Caron et al. [17], Coutier-Delgosha et al. [18], de Lange et al. [19], Leroux et al. [20], Callenaere et al. [21] and Reboud et al. [23]).

1.3.3 Velocity on the Boundary Between the Liquid and Vapor v_i

Based on a steady Bernoulli equation one can assume that the velocity of the reentrant jet will be equal to interface velocity. Only Bachert et al. [13] and Frobenius et al. [14] (in a common study) used this velocity that is in close relation to the cavitation cloud shedding. This was only made possible by complicated and expensive PIV measurements in cavitating flow. Using this value for characteristic velocity has, therefore, little potential for a broader use within the scientific community.

1.3.4 Corrected Free Stream Velocity v_σ

It is obvious that defining velocity on the boundary between cavitation and liquid is very complicated and can only be determined by expensive and complicated PIV (Sec. 3.2) or maybe two optical probe (Stutz and Reboud [15]) measurements. Therefore, several authors (Laberteaux and Ceccio [22], Hofman et al. [24] and de Lange and de Bruin [25]) used an approximation of the interface (reentrant jet) velocity, defined as:

$$v_\sigma = v_\infty \cdot \sqrt{1 + \sigma}, \quad (2)$$

where v_∞ is the velocity upstream of the hydrofoil and σ is the cavitation number (Eq. 3).

In essence, this relation (Eq. 2) acknowledges the presence of the cavitation structure, which is left out when only the free stream velocity is used (Sec. 1.3.2).

2 EXPERIMENT

The experiment was set up in a cavitation tunnel at the Laboratory for Turbomachinery and Fluid Power – Darmstadt University of Technology. High speed camera visualization and PIV measurements were performed to show the vast span of Strouhal numbers that can be associated with a single well-defined experiment and finally, to support the proposed definition of the Strouhal number. The PIV measurements were described in detail and discussed in several papers – for example Dular et al. [26] so only a brief overview will be given here.

Two simple hydrofoils were used. The basic geometry is a 50 mm wide, 107.9 mm long and 16 mm thick symmetric hydrofoil with a circular leading edge and parallel walls. To further investigate the complicated flow phenomena and to obtain some three-dimensional cavitation effects the basic geometry was modified by sweeping back the leading edge at an angle of 15 (Asymmetric Leading Edge hydrofoil – ALE15) and 25 degrees (ALE25) (Fig. 4).

The velocity in the reference plane upstream of the hydrofoil was held constant at 13 m/s ($Re = 1.38 \cdot 10^6$ based on the chord length). Developed cavitating flow was observed at an incidence angle of 5° and at cavitation numbers $\sigma = 2.0, 2.3$ and 2.5 .



Fig. 4. ALE15 and ALE25 hydrofoils

The cavitation number σ is calculated on the base of the pressure at the inlet of the test section p_∞ (measured at the position 400 mm upstream from the hydrofoil) and on the vapor pressure p_v (at system temperature) divided by the dynamic pressure (defined by fluid density ρ and upstream flow velocity v_∞):

$$\sigma = \frac{p_\infty - p_v}{\rho \cdot v_\infty^2 / 2}. \quad (3)$$

2.1 High Speed Visualization

Images of cavitation structures were captured from the side view by a high speed Sencam PCO digital CCD camera. The image capturing frequency was 1826 fps at a resolution of 1024·256 pixels in 8 bit color resolution. The internal memory of the camera is 512 MB which, together with images size of about 1 MB, limited the time and the number of recorded images in the sequence to about 0.3 s and 600 images, respectively. The expected maximal frequency of cavitation cloud shedding was about 400 Hz which meant that approximately 130 cycles would be recorded. This was more than enough for a statistical evaluation and FFT analysis.

Fig. 5 shows a sequence of cavitation cloud shedding on the ALE15 hydrofoil at $v_\infty = 13$ m/s and $\sigma = 2.3$.

The first image shows the attached part of the cavity and a separated cavitation cloud downstream. The attached cavity grows until the new cavitation cloud separates (in Fig. 5). The cloud then travels downstream and collapses in a higher pressure region (in Fig. 5). Meanwhile, the attached cavity grows and a new separation occurs.

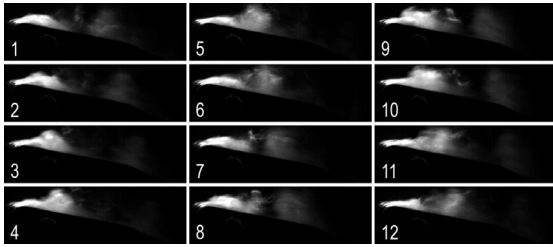


Fig. 5. A sequence of cavitation cloud shedding

To determine the shedding frequency FFT analysis of the images was made. A region of interest was selected in the image (downstream of the maximum attached cavity length) where the evaluation then took place.

Characteristic lengths were determined either by measuring the hydrofoil or from the images. A threshold value that defined the boundary of the cavitation structure was chosen – cavitation structures are characterized by a high value of gray level (bright region) in the recorded image. The boundary of the cavitation structure in each image was considered to be the isoline of a certain gray level (128 (50 % brightness)); the pixels in the image in 8 bit resolution can occupy values from 0 (black) to 255 (white).

A time or phase averaged cavity shape was determined by averaging the cavitation structure boundary data from each image.

The value of the threshold somewhat influences the value of the measured length. Tests with 25 and 75 % brightness were performed – the determined length varied a bit, but the trend remained the same, which is of the greatest importance in calculating nondimensional numbers. Moreover, the gradient in the gray level between the vapour structures and surroundings in the images is relatively large, resulting in a small influence of the threshold value.

2.2 PIV Measurements

As mentioned above, a detailed description of the procedure and the methods that were used can be found in Dular et al. [26]. A combination of PIV measurements with LIF (Laser Induced Fluorescence) technique made it possible to obtain the information about the velocity field outside and inside the cavitation pocket on the hydrofoil. Fluorescent tracer particles were added to the water as seed. When light at a wavelength of 532 nm (green spectrum) illuminates them they emit light at a wavelength of 590 nm (yellow

spectrum). By fitting the CCD-camera with an appropriate light it is possible to get suitable images of the tracer particles for the PIV analysis. Since the camera records only the light in the yellow spectrum, the cavitation structure is filtered out of the image and tracer particles inside it can also be detected.

Fig. 6 shows the measured instantaneous velocity field just after the separation of cavitation cloud (ALE15 hydrofoil at $v_{\infty} = 13$ m/s and $\sigma = 2.3$).

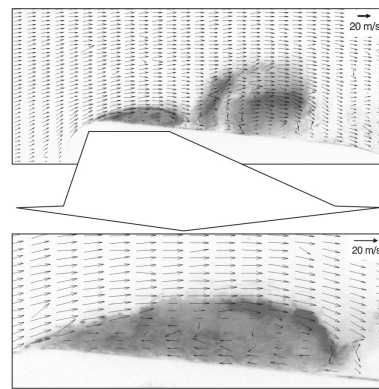


Fig. 6. Instantaneous velocity field

The bottom image shows the magnification of the situation where the velocity field around the attached cavity closure is well seen. The velocities on the interface and of the reentrant jet indeed lie in the same order of magnitude and reach up to about 20 m/s.

Free stream and corrected free stream velocity determination is straightforward. The reentrant jet and interface velocities (phase averaged velocities) were determined from PIV-LIF data.

3 RESULTS

The values for all the interpretations of characteristic variables that were found in the literature survey and are described in Sec. 2 were determined for the six experiments that were performed. Tables 1 to 3 give the values for the characteristic frequency, length and velocity respectively. In addition to the interpretations that were found in references the most appropriate values – the mean length of the separated cavitation cloud l_{cc} and the reentrant jet velocity v_{ij} were determined from the experiments.

Table 1. *Shedding frequencies for the investigated cavitation conditions*

	f [Hz]
ALE15, $\sigma = 2.0$	190
ALE15, $\sigma = 2.3$	303
ALE15, $\sigma = 2.5$	366
ALE25, $\sigma = 2.0$	259
ALE25, $\sigma = 2.3$	330
ALE25, $\sigma = 2.5$	442

Table 2. *Characteristic lengths for the investigated cavitation conditions*

	l_h [m]	l_{ht} [m]	l_{ct} [m]	l_c [m]	l_{ac} [m]	l_{cc} [m]
ALE15, $\sigma = 2.0$	0.1079	0.016	0.013	0.077	0.038	0.028
ALE15, $\sigma = 2.3$	0.1079	0.016	0.013	0.068	0.026	0.022
ALE15, $\sigma = 2.5$	0.1079	0.016	0.011	0.055	0.021	0.016
ALE25, $\sigma = 2.0$	0.1079	0.016	0.013	0.063	0.037	0.031
ALE25, $\sigma = 2.3$	0.1079	0.016	0.011	0.054	0.033	0.023
ALE25, $\sigma = 2.5$	0.1079	0.016	0.008	0.046	0.027	0.015

Table 3. *Characteristic velocities for the investigated cavitation conditions*

	v_∞ [m/s]	v_i [m/s]	v_σ [m/s]	v_{rj} [m/s]
ALE15, $\sigma = 2.0$	13	19.9	22.5	18.3
ALE15, $\sigma = 2.3$	13	19.3	23.6	18.4
ALE15, $\sigma = 2.5$	13	19.1	24.3	17.4
ALE25, $\sigma = 2.0$	13	20.2	22.5	17.7
ALE25, $\sigma = 2.3$	13	19.4	23.6	17.8
ALE25, $\sigma = 2.5$	13	19.3	24.3	16.2

As expected, the cavitation cloud shedding frequencies increase when the cavitation number decreases. The order of magnitude of the shedding frequency is mainly a function of the hydrofoils shape – as anticipated the highest frequency in an order of 400 Hz. The listed

frequency values are the mean values – the average deviation is about $\pm 7\%$.

When the characteristic length had to be determined from the cavitation image (l_{ct} , l_c , l_{ac} and l_{cc}) computer aided visualization was employed to minimize the human factor (Sec. 3.1) – the uncertainty was therefore, reduced to the color and size resolution of the images. Apart from the hydrofoil dimensions (l_h and l_{ht}), which was measured with great accuracy, we estimated that the characteristic lengths were determined with an uncertainty of about $\pm 5\%$.

The free stream velocity v_∞ was measured by inductive flow meter Fischer & Porter D10D with uncertainty of 1% of the measured value (the uncertainty of the channel cross-section measurement is marginal). The cavitation number could be determined with a global uncertainty of ± 0.04 , which leads to uncertainty of the corrected free stream velocity v_∞ of about $\pm 2.5\%$. We estimated that the velocities derived from the PIV data (v_i and v_{rj}) are correct within $\pm 5\%$.

Considering the combination of inaccuracies of frequency, length and velocity measurements the Strouhal number (for the worst possible case where the length was measured from the image and the velocity from the PIV data) was determined with an uncertainty of $\pm 10\%$ of the measured value.

If we compare only the combinations of variables that have been used in past studies we get the results presented in Table 4. The most appropriate values of Str number determined from the mean length of the separated cavitation cloud l_{cc} and the reentrant jet velocity v_{rj} are included for reference.

The results from Table 4 are additionally presented in the diagram in Fig. 7. The bold line without markers represents Str numbers that were calculated on the basis of the mean length of the separated cavitation cloud l_{cc} and the reentrant jet velocity v_{rj} (the correct »reference« values).

It is obvious that great discrepancies in the calculated value of the Str number exist when different interpretations are used. The difference between the correct »reference« value (calculated by use of l_{cc} and v_{rj}) and the worst selection can be almost one order of magnitude (case of ALE15 hydrofoil at $\sigma = 2.5$ and ALE25 hydrofoil at $\sigma = 2.5$ – correct value equals 0.34 (ALE15) and 0.41 (ALE25), calculation according to [4] and [6] to [10] gives 3.04 (ALE15) and 3.67 (ALE25)).

Table 4. Values for Str number according to the definitions found in literature

l	v	Str (ALE15, $\sigma = 2.0$)	Str (ALE15, $\sigma = 2.3$)	Str (ALE15, $\sigma = 2.5$)	Str (ALE25, $\sigma = 2.0$)	Str (ALE25, $\sigma = 2.3$)	Str (ALE25, $\sigma = 2.5$)	Reference
l_{cc}	v_{rj}	0.29	0.36	0.34	0.45	0.43	0.41	CORRECT VALUE
l_h	v_∞	1.58	2.51	3.04	2.15	2.74	3.67	[4, 6-10]
l_{ht}	v_∞	0.23	0.37	0.45	0.32	0.41	0.54	[11]
l_{ct}	v_∞	0.19	0.30	0.31	0.26	0.28	0.27	[12]
l_c	v_i	0.74	1.07	1.05	0.81	0.92	1.05	[13, 14]
l_c	v_∞	1.13	1.58	1.55	1.26	1.37	1.56	[15, 16]
l_{ac}	v_∞	0.56	0.61	0.59	0.74	0.84	0.92	[4, 5, 8, 17-21, 23]
l_{ac}	v_σ	0.32	0.33	0.32	0.43	0.46	0.49	[22, 24, 25]

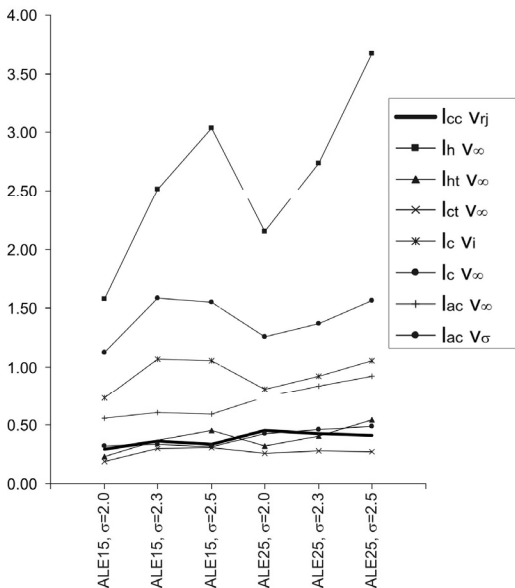


Fig. 7. Values for Str number according to the definitions found in literature

The most frequently used definition uses frequency f , the mean attached cavity length l_{ac} and free stream velocity v_∞ and sets the value of Str number to about twice too high for all the cases. A very frequently used combination with the hydrofoil length l_h and free stream velocity v_∞ as reference values is unacceptable – the values significantly differ from the correct value and also show an incorrect trend. It can also be seen that some combinations produce a relatively accurate result although this may be more a case of luck than the most suitable selection of

variables (for example choosing the hydrofoil thickness l_{ht} as the characteristic length).

It is obvious that a vast span of results can be achieved when different interpretations for characteristic variables are used. Besides using the mean length of the separated cavitation cloud l_{cc} and the reentrant jet velocity v_{rj} – variables that demand using costly PIV and visualization techniques – the most appropriate and also relatively easy to determine the combination of variables is the mean length of the attached part of the cavity l_{ac} and the corrected free stream velocity v_σ .

To further emphasize the necessity to unify the definition of Str number as the measure of cavitating flow dynamics and as the reference for accuracy of simulations, results of all possible combinations of variables for the case of ALE15 hydrofoil at $\sigma = 2.3$ are presented in Table 5.

It is obvious that an appropriate combination of variables will give almost any result of Strouhal number – the span of values for the case in question (ALE15 hydrofoil at $\sigma = 2.3$) reaches from 0.17 to 2.51, which is more than one order of magnitude.

Table 5. Strouhal numbers for calculated with different characteristic quantities

	l_h	l_{ht}	l_{ct}	l_c	l_{ac}	l_{cc}
v_∞	2.51	0.37	0.30	1.58	0.61	0.51
v_i	1.69	0.25	0.20	1.07	0.41	0.35
v_σ	1.38	0.21	0.17	0.87	0.33	0.28
v_{rj}	1.78	0.26	0.21	1.12	0.43	0.36

4 CONCLUSIONS

The study showed that there is a great inconsistency in the definition of the Strouhal number when defining the dynamics of the developed cavitating flow. It was also shown that when variables in a strict relation with the cavitation cloud shedding are used, the value of Strouhal number lies within the expected range. Other, easier to determine, quantities set it to a more or less accurate value. The study also showed that some frequently used quantities like hydrofoil length or the mean length of cavitation structure are inappropriate to use.

In order to avoid confusion, misinterpretation or even manipulation of results, it should therefore, be essential to use only one definition for the Str number to describe the dynamics of the cavitating flow. Such a demand cannot be easily made since in many cases some variables are hard or even impossible to determine. But in other cases where visual access to the cavitation is available, the combination of shedding frequency f , mean attached cavity length l_{ac} and corrected free stream velocity v_σ should be used to define the Strouhal number:

$$Str = \frac{f \cdot l_{ac}}{v_\sigma} = \frac{f \cdot l_{ac}}{v_\infty \sqrt{1 + \sigma}} \quad (4)$$

Finally, in cases where there is no visual access or other method available to determine the mean length of the attached part of the cavity, the need to include a clear definition of Str number remains.

5 NOMENCLATURE

f	characteristic frequency
l	characteristic length
l_{ac}	the mean length of the attached part of the cavity
l_c	the mean cavity length
l_{cc}	the mean length of the separated cavitation cloud
l_{ct}	the mean cavity thickness
l_h	hydrofoil length
l_{ht}	maximum thickness of the hydrofoil
p_v	vapour pressure
Str	Strouhal number
v	characteristic velocity
v_i	velocity on the boundary between the liquid and vapor

v_{rj}	reentrant jet velocity
v_σ	corrected free stream velocity
v_∞	free stream velocity
σ	cavitation number

6 REFERENCES

- [1] Kunz, R.F., Lindau, J.W., Billet, M.L., Stinebring, D.R. (2001), Multiphase CFD modeling of developed and supercavitating flows, Defense Technical Information Center, Compilation Part Notice ADP012082.
- [2] Kawamura, T., Sakoda, M. (2003), Comparison of bubble and sheet cavitation models for simulation of cavitating flow over a hydrofoil, Proc. of the Fifth International Symposium on Cavitation, Osaka.
- [3] Hosangadi A., Ahuja V. (2006), A numerical study of cavitation in cryogenic fluids part II: new unsteady model for dense cloud formation, Proc. of the Sixth International Symposium on Cavitation, Wageningen.
- [4] Saito, Y., Nakamori, I., Iko-hagi, T. (2003), Numerical analysis of unsteady vaporous cavitating flow around a hydrofoil, Proc. of the Fifth International Symposium on Cavitation Osaka.
- [5] Franc, J.P. (2001), Partial cavity instabilities and re-entrant jet, Proc. of the Fourth International Symposium on Cavitation, Pasadena.
- [6] Duttweiler, M.E., Brennen, C.E. (1998), Partial cavity instabilities, Proc. of US-Japan seminar: Abnormal flow phenomena in turbomachines, Osaka.
- [7] Schnerr, G.H., Sauer, J. (2001), Physical and numerical modelling of unsteady cavitation dynamics, Proc. of the Fourth International Conference on Multiphase Flow, New Orleans.
- [8] Iga, Y., Nohmi, M., Goto, A., Shin, B.R., Iko-hagi, T. (2003), Numerical study of sheet cavitation breakoff phenomenon on a cascade hydrofoil, Journal of Fluids Engineering, no. 125, p. 643-651.
- [9] Sato, K., Tanada, M., Monden, S., Tsujimoto, Y. (2001), Observations of oscillating cavitation on a flat plate hydrofoil, Proc. of the Fourth International Symposium on Cavitation, Pasadena.

- [10] Song, C.C.S., Qin, Q. (2001), Numerical simulation of unsteady cavitating flows, Proc. of the Fourth International Symposium on Cavitation, Pasadena.
- [11] Berntsen, G.S., Kjeldsen, M., Müller, R. (2001), Cavitation induced dynamics in hydraulic machinery, Proc. of the 10th International Meeting of the Work Group on the Behaviour of Hydraulic Machinery Under Steady Oscillatory Conditions, Trondheim.
- [12] Ceccio, S.L., Brennen, C.E. (1992), Dynamics of attached cavities on bodies of revolution, Journal of Fluids Engineering, no. 114, p. 93-99.
- [13] Bachert, R., Ludwig, G., Stoffel, B., Frobenius, M., Schilling, R. (2003), Three-dimensional unsteady cavitation effects on a single hydrofoil and in a radial pump - measurements and numerical simulations; part one: experiments, Proc. of the Fifth International Symposium on Cavitation, Osaka.
- [14] Frobenius, M., Schilling, R., Bachert, R., Stoffel, B., Ludwig, G. (2003), Three-dimensional unsteady cavitation effects on a single hydrofoil and in a radial pump - measurements and numerical simulations, part two: numerical simulation, Proc. of the Fifth International Symposium on Cavitation, Osaka.
- [15] Stutz, B., Reboud, J.L. (1997), Experiments on unsteady cavitation, Experiments in Fluids, no. 22, p. 191-198.
- [16] Maître, T., Pellone, C. (2001), Numerical modelling of unsteady partial cavities behind a backward facing step, Proc. of the Fourth International Symposium on Cavitation, Pasadena.
- [17] Caron, J.F., Farhat, M., Avellan, F. (1999), The influence of flow unsteadiness on erosive cavity dynamics, Proc. of the Third ASME/JSME Joint Fluids Engineering Conference, San Francisco.
- [18] Coutier-Delgosha, O., Fortes-Patella, R., Reboud, J.L. (2003), Evaluation of turbulence model influence on the numerical simulations on unsteady cavitation, Journal of Fluids Engineering, no. 125, p. 38-45.
- [19] de Lange, D.F., de Bruin, G.J., van Wijngaarden, L. (1994), Observations of cloud cavitation on a stationary 2D profile, Bubble Dynamics and Interface Phenomena, Kluwer Academic Publishers, p. 241-246.
- [20] Leroux, J.B., Coutier-Delgosha, O., Astolfi, J.A. (2003), A joint experimental and numerical study of mechanisms associated to instability of partial cavitation on two-dimensional hydrofoil, Proc. of the Fifth International Symposium on Cavitation, Osaka.
- [21] Callenaere, M., Franc, J.P., Michel, J.M., Riondet, M. (2001), The cavitation instability induced by the development of a re-entrant jet, Journal of Fluid Mechanics, no. 444, p. 223-256.
- [22] Laberteaux, K.R., Ceccio, S.L. (2001), Partial cavity flows, part 1. Cavities forming on models without spanwise variation, Journal of Fluid Mechanics, no. 431, p. 1-41.
- [23] Reboud, J.L., Coutier-Delgosha, O., Pouffary, B., Fortes-Patella, R. (2003), Numerical simulation of unsteady cavitating flows: some applications and open problems, Proc. of the Fifth International Symposium on Cavitation Osaka.
- [24] Hofmann, M., Lohrberg, H., Ludwig, G., Stoffel, B., Reboud, J.L., Fortes-Patella, R. (1999), Numerical and experimental investigations on the self - oscillating behaviour of cloud cavitation - Part 1: Visualisation, Proc. of the Third ASME / JSME Joint Fluids Engineering Conference, San Francisco.
- [25] de Lange, D.F., de Bruin, G.J. (1998), Sheet cavitation and cloud cavitation, re-entrant jet and three-dimensionality, Applied scientific research, no. 58, p. 91-114.
- [26] Dular, M., Bachert, R., Stoffel, B., Širok, B. (2005), Transient simulation, visualization and PIV-LIF measurements of the cavitation on different hydrofoil configurations, Strojniški vestnik - Journal of Mechanical Engineering, vol. 51, no.1 , p. 13-27.